ASSESSING THE ROLE OF ANHYDRITE IN THE KT MASS EXTINCTION: HINTS FROM SHOCK-LOADING EXPERIMENTS. R. Skála[1], F. Langenhorst[2] and F. Hörz[3], [1]Czech Geological Survey, Klárov 3/131, CZ-118 21 Praha 1, Czech Republic, skala@cgu.cz, [2]Bayerisches Geoinstitut (BGI), University of Bayreuth, D-95440 Bayreuth, Germany, [3]NASA-JSC, SN-2, Houston, Texas 77058, USA.

Introduction: Various killing mechanisms have been suggested to contribute to the mass extinctions at the KT boundary, including severe, global deterioration of the atmosphere and hydrosphere due to SO_x released from heavily shocked, sulfate-bearing target rocks [1-6]. The devolatilization of anhydrite is predominatly inferred from thermodynamic considerations [4-6] and lacks experimental confirmation. To date, the experimentally determined shock behavior of anhydrite is limited to solid-state effects employing X-ray diffraction methods [7-9]. The present report employs additional methods to characterize experimentally shocked anhydrite.

Experimental: Massive polycrystalline anhydrite was placed into metal jackets and shock-loaded using a 20-mm-caliber powder gun at NASA-JSC [e.g. 7]. Peak shock pressures attained by multiple reverberations ranged from 4 to 64 GPa. The recovered samples were examined by optical microscopy, scanning (SEM) and transmission electron microscopy (TEM), and X-ray powder diffraction to characterize the solid-state shock behavior of anhydrite.

Results: *Optical microscopy.* At hand-specimen scales, the unshocked anhydrite was massive and non-porous, with individual grains being clear and transparent. In thin section, this material consists largely of subhedral to anhedral anhydrite grains (typically ~ 0.3-0.5 mm across) and mosaic texture. Anhydrite grains frequently display cleavage and some grains are twinned. Samples recovered from the metal containers after shock loading are pervasively fractured and generally disintegrate easily. Individual grains are white, and non-transparent. In thin section, the shocked samples are strongly fragmented. They display more cleavage planes than the unshocked material. Commonly, fracturing along two perpendicular cleavage systems occurs, resulting in a jagged appearance of grain boundaries. Undulatory extinction is pervasive in the shocked samples. Twinning is more frequent in shocked samples compared to the starting material and of different appearance. The twins in the unshocked material form relatively wide, rectangular lamellae with straight boundaries, often extending across the entire grain. In contrast, the twins in the shock-loaded anhydrite form narrow, needle-shaped, lenticular parallel domains. Samples shocked to pressures above 50 GPa contain grains of peculiar appearance that seem to be composed of fibrous, felt-like aggregates and that display low birefringence colors (gray and white-gray).

Scanning electron microscopy. Back-scattered electron (BSE) as well as secondary electron (SE) imaging revealed a number of shock-induced defects. In BSE images, samples shock-loaded to 4 GPa display high numbers of parallel cleavage planes. Also, irregular fractures, cross-cutting the anhydrite crystals into a mosaic of grains, sometimes less than a few microns in diameter, are present in these low pressure experiments. The number of fractures or the size of associated fragments, however, cannot easily be correlated with peak shock pressure because of the somewhat heterogeneous distribution of shock effects throughout the volume of the sample; some regions display more severe deformation than others.

The secondary electron images display relatively narrow bands of heavy comminution at all pressures. The fragments in these zones are usually irregular in shape, with sizes frequently a few microns across. These grains only occasionally display cleavage planes in more than one direction, but the fracture pattern may also be completely irregular. In some samples narrow zones with multiple cross-cut cleavages occur. Often, shock-loaded samples display a "scaly" fabric consisting of remarkably thin and flat grains. This distinct fabric is most likely due to the extremely good cleavage of anhydrite.

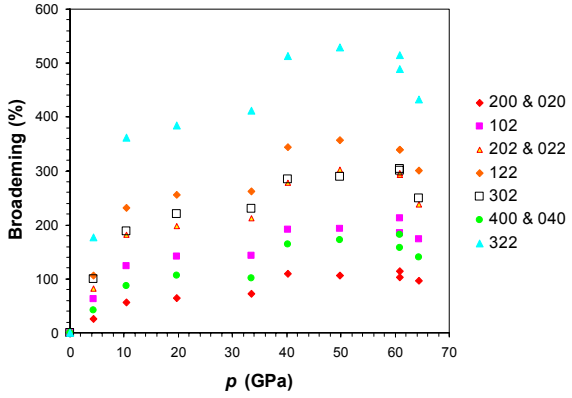

Fig. 1. *Relative broadening of selected reflections (indexed in the Amma setting of the space group).*

X-ray diffraction. All X-ray powder diffraction patterns yielded anhydrite as a dominant phase. Insignificant extra peaks were found to be consistent with trace amounts of gypsum, dolomite and/or quartz. This

agrees well with chemical data acquired with SEM and TEM. The unit-cell dimensions, refined from the positions of ten most prominent, non-overlapping diffraction lines, deviate by less than 0.15 % from the nominal values. Line broadening, however, is prominent already at 4 GPa and increases systematically with pressure, albeit not linearly, up to 50 GPa. Above this limit the broadening decreases slightly (see Fig. 1).

Transmission electron microscopy. Transmission electron microscopy revealed that the starting material is almost free of any defects. Next to rare growth twins and cleavage fractures parallel to (001) and (010), it does contain rare straight dislocations (in the (010) glide plane; density $\leq 10^8$ m^{-2}). In contrast, the shocked anhydrite contains many deformation features, even at low pressures. These include mainly dislocations and twins. Straight dislocations are typical for the unshocked material and for samples shocked to less than 30 GPa, but the density of dislocations is markedly higher in shock-loaded material, reaching about 10^{13} m^{-2} at 4 GPa and 10^{14} m^{-2} at 33 GPa. At higher pressures, dislocations are polygonized (Fig. 2). At the same time some areas appear that are completely devoid of dislocations, possibly corresponding to regions of elevated post-shock temperatures and the onset of some annealing. The twins in the shocked material occur as relatively thin lamellae. So-called Rose channels due to a multiple twinning have been identified in the sample shock-loaded to 20 GPa.

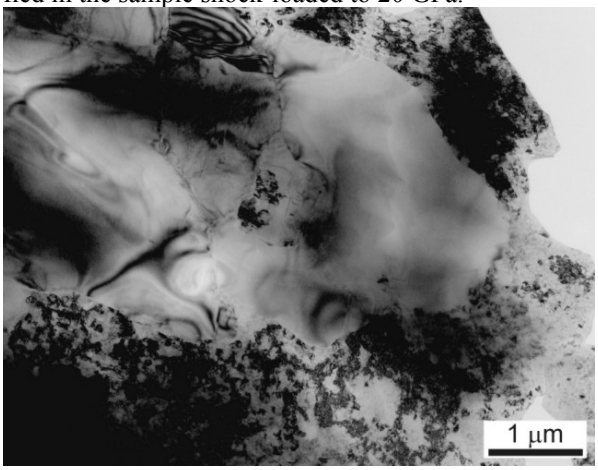

Fig. 2. *Bright-field TEM image of highly (61 GPa) shocked anhydrite showing defect-free areas that have crystallized from the quenched melts. Coexisting defect-rich grains show polygonization of dislocations.*

Samples shock-loaded to 60 GPa and above display melting. At 61 GPa some shear zones appear to be filled with quenched melt (Fig. 3) and some irregular melt pockets have formed (Fig. 2). The shear zones are typically ~ 100-200 nm wide being parallel to cleavage planes. At 64 GPa melting seems to be pervasive. In highly deformed materials of the 64 GPa sample, some rare bubbles have been found, but no decomposition products have been identified that could possibly relate to outgassing.

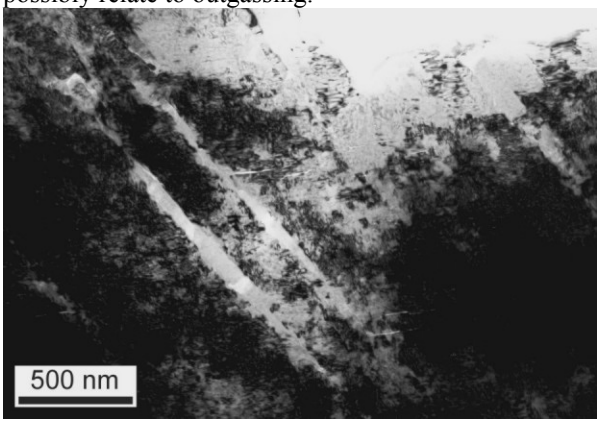

Fig. 3. *Bright-field TEM image of highly (61 GPa) shocked anhydrite displaying shear zones filled with quenched melt.*

Conclusions: Shocked anhydrite displays a number of defects, including twinning, dislocations as well as shear zones mostly along cleavage planes. No changes in the phase composition have been observed. Unit-cell dimensions vary by less than 0.15 rel. % over a wide range of shock pressures. Also, neither high-pressure polymorphs nor any decomposition products have been found in the experimentally shocked anhydrite, indicating that anhydrite is rather stable under the conditions simulated by our experiments. The coexistence of highly deformed regions with regions free of dislocations indicates that some annealing must have taken place. Melting seems, at least at lower pressures, to be associated with shearing; this suggests that whole-scale devolatilization proposed by several models is not necessarily a major process, even at the highest pressures accomplished in our dynamic loading experiments. Gradual narrowing of XRD-peaks above 50 GPa is consistent with the TEM observations of quenched anhydrite melts.

Acknowledgments. Data for this presentation have been collected when RS was an EU Marie Curie Programme Fellow at the Bayerisches Geoinstitut, Universität Bayreuth, Bayreuth, Germany.

References: [1] Emiliani C. et al. (1981) *EPSL, 55*, 317-334. [2] Brett R. (1992) *GCA, 56*, 3603-3606. [3] Sigurdsson H. et al. (1992) *EPSL, 109*, 543-559. [4] Chen G. et al. (1994) *EPSL, 128*, 615-628. [5] Yang W. and Ahrens T. J. (1998) *EPSL, 156*, 125-140. [6] Gupta S. et al. (2001) *EPSL, 188*, 399-412. [7] Schmitt R.T. and Hornemann U. (1998) *LPS XXIX*, Abstract # 1019. [8] Langenhorst F. et al. (2003) *LPS XXXIV*, Abstract #1638. [9] Skála R. et al. (2003) 3rd Large Meteorite Impacts Conference, Abstract #4093.